ed., edited by K. H. Hellwege (Springer-Verlag, Berlin, 1955), Part 4.
[32]*Handbook of Physics*, 2nd ed., edited by E. U. Condon and H. Odishaw (McGraw-Hill, New York, 1967).
[33]V. Heine, J. Phys. C 1, 222 (1968).

PHYSICAL REVIEW B VOLUME 3, NUMBER 12 15 JUNE 1971

Model-Potential Calculations of Phonon Energies in Aluminum

W. M. Hartmann* and T. O. Milbrodt†
Physics Department, Michigan State University, East Lansing, Michigan 48823
(Received 14 January 1971)

The calculation of the lattice dynamics of simple metals to second order in a local model potential is discussed in terms of the real-space sum of Born–von Karman central-force constants. The real-space sum is found to converge faster than the more common reciprocal-space sum and to be more convenient for the calculation of thermal properties and integral properties of the electron-phonon interaction. The reciprocal-space sum is more suitable for the calculation of Kohn anomalies and elastic constants and may be generalized to more complicated models of the electron-ion interaction. These points are illustrated by a calculation of aluminum phonon energies throughout the Brillouin zone. Excellent agreement of the calculated dispersion relations along 10 symmetry lines, density of states, and specific heat with the experimental quantities are obtained by fitting the two parameter Harrison potential and using the Toigo-Woodruff susceptibility function. The results from this model are compared with those from the two models used by Wallace and with those of the eight-shell force-constant fit by Gilat and Nicklow. The predictions of the three models for band structure and for electrical resistivity of the liquid are discussed.

I. INTRODUCTION

Since the early calculations by Toya[1] and Cochran[2] of the lattice dynamics of Na, numerous calculations have been made of the elastic properties of simple metals based upon the pseudopotential or model-potential approach to the electron-ion interaction. Calculations have been reported for the alkali metals,[3–22] for Al;[17–21,23–26] for the hexagonal metals Be, Mg, and Zn,[20,27–34] for Pb,[21,22,35,36] and for Sn.[37]

The dynamical matrix from which phonon energies and polarization vectors are calculated may be obtained either by summing real-space force constants or by performing a sum in reciprocal space. To our knowledge the real-space sum has not previously been used in a complete calculation from first principles, though Cochran[2] used it to determine an ion-electron-ion interaction from phonon dispersion curves, and Shyu and Gaspari[4,18] have calculated force constants.

In Sec. II the real-space and k-space sums are discussed and compared. In Sec. III three models for the interionic potential are presented and the pseudopotentials are tested against band-structure and liquid-resistivity data. Of these three models two are those of Wallace,[24] and the third uses a susceptibility function derived by Toigo and Woodruff. In Sec. IV the real-space sum is used to calculate phonon dispersion relations, density of states, and lattice specific heat for the models of Sec. III.

II. REAL- AND RECIPROCAL-SPACE METHODS

If the pseudopotential is local, the effects of the ion-electron-ion interaction may be incorporated into a simple two-body interionic potential $V(R)$ which then may be written as the sum of direct Coulomb and band-structure terms

$$V(R) = Z^2e^2/R + V^{\mathrm{bs}}(R) ,$$

where the band-structure contribution is given by

$$V^{\mathrm{bs}}(R) = -(2\pi)^{-3}\int d^3q\, e^{i\vec{q}\cdot\vec{R}}\left(\frac{4\pi Z^2e^2}{q^2}\,C(q)\right)$$

$$= \frac{-2Z^2e^2}{\pi}\int C(q)\frac{\sin(qR)}{qR}\,dq . \qquad (2.1)$$

The function $C(q)$ is the ratio of the Fourier transform of the ion-electron-ion interaction to that of the direct Coulomb interaction; it was introduced by Cochran and is a useful interface between the electronic and the phonon calculations. The dynamical matrix is given in the central-force or axially symmetric model, in which the force between two ions depends only upon the distance between them, by

$$D_{\alpha\beta}(\vec{k}) = \sum_l (1 - e^{-i\vec{k}\cdot\vec{R}_l})\frac{\partial^2}{\partial R_\alpha \partial R_\beta}\,V(R)\Big|_{\vec{R}=\vec{R}_l} , \qquad (2.2)$$

where $R_{l\alpha}$ is the αth Cartesian component of the position vector of the lth ion.

The differentiation in (2.2) is commonly done in one of two ways. A real-space sum for $\overleftrightarrow{D}(\vec{k})$ is obtained by defining radial ($\mathcal{R}$) and tangential ($\mathcal{T}$) force constants, which depend only upon the distance between ions,

$$\mathcal{T}_l = R^{-1}\frac{\partial V}{\partial R}\bigg|_{R_l} = -\frac{Z^2e^2}{R_l^3} - \frac{2Z^2e^2}{\pi R_l^2} \times \int_0^\infty C(q)\left(\cos qR_l - \frac{\sin qR_l}{qR_l}\right) dq \,, \tag{2.3}$$

$$\mathcal{R}_l = \frac{\partial^2 V}{\partial R^2}\bigg|_{R_l} = -2\mathcal{T}_l + \frac{2Z^2e^2}{\pi R_l}\int_0^\infty C(q)\, q \sin qR_l\, dq \,.$$

From (2.3) and (2.2)

$$D_{\alpha\beta}(\vec{k}) = \sum_l (1 - e^{i\vec{k}\cdot\vec{R}_l})[\mathcal{T}_l\delta_{\alpha\beta} + (R_{l\alpha}R_{l\beta}/R_l^2)(\mathcal{R}_l - \mathcal{T}_l)]\cdot$$

Alternatively, the band-structure contribution to the potential can be differentiated in the Fourier-transformed form (2.1), the sum over all real-lattice sites can be exactly done, and one obtains a sum over reciprocal-lattice vectors $\vec{H}$

$$D^{bs}_{\alpha\beta}(\vec{k}) = \frac{4\pi Z^2e^2N}{\Omega}\left(\sum_{\vec{H}}\frac{(\vec{k}+\vec{H})_\alpha(\vec{k}+\vec{H})_\beta}{|\vec{k}+\vec{H}|^2} \times C(|\vec{k}+\vec{H}|) - \sum_{\vec{H}\neq 0}\frac{H_\alpha H_\beta}{H^2}C(H)\right). \tag{2.4}$$

The Coulomb contribution is then included by performing the Kellermann sum.[38]

Previous authors have used the latter method, which has the advantage of relating the dynamical matrix elements rather directly to the function $C(q)$. The reciprocal-space sum has the additional advantage that it may be readily generalized to cases of nondiagonal electron-gas susceptibility functions[39,40] for which a central two-body potential is not a natural representation of the ion-electron-ion interaction. This method has the disadvantage that the entire calculation must be done anew for each value of the wave vector $\vec{k}$. This feature is not usually a serious problem if only dispersion curves along symmetry directions are wanted, but might pose a computer time problem in calculating lattice-thermal properties or aspects of the electron-phonon interaction where phonon energies and polarization vectors over the whole Brillouin zone are needed. Particular difficulty might occur at large electron densities where the sum over reciprocal-lattice vectors converges slowly. A sphere in reciprocal space of radius ck_F contains approximately $N_H \approx \frac{1}{2}Zc^3$ reciprocal-lattice points for cubic structures. Wallace, however, has successfully performed thermodynamic calculations for Al using the reciprocal-space sum, although he required a sphere of radius 20 k_F, $N_H \approx 12\,000$ points.[24,26] The advantage of the real-space method is that once a set of interionic force constants is determined, it is relatively easy to calculate lattice properties depending on all $\vec{k}$ by interpolation schemes such as that of Gilat and Dolling, and Gilat and Raubenheimer.[41]

The function $C(q)$, summed over the reciprocal lattice, is proportional to the electron-gas susceptibility at large q, and hence decays as q^{-4}. Since the force constants, summed over the real lattice, decay as R^{-5}, one might expect the real-space sum to converge somewhat faster for large phonon wave vectors. If the reciprocal-space sum is used, poor convergence may be recognized by the energy gaps which occur at wave vectors where several phonons ought to be degenerate by symmetry. By contrast, both translational and point symmetries are retained in all shells of the real-space sum. This fact may, however, be an advantage if one is calculating electron-phonon interaction matrix elements for Fermi surfaces which extend beyond the first Brillouin zone.[42]

Although we shall show that the real-space sum offers a reasonable alternative for calculations of smooth dispersion curves, this method is quite hopeless for calculation of such rapidly varying aspects as Kohn anomalies. The Kohn anomaly appears in only one term of Eq. (2.4) (or in several for $\vec{k}$ at a symmetry point), whereas every term of the real-space sum includes part of the anomaly. For a spherical Fermi surface the function $C(q)$ has a singular derivative at $q = 2k_F$, so that for some reciprocal-lattice vector $\vec{H}_0$ the contribution to the dynamical matrix has a singular derivative

$$\frac{\partial D^0(k)}{\partial k} \sim \ln\left|1 - \frac{|\vec{k}-\vec{H}_0|}{2k_F}\right|, \quad |\vec{k}-\vec{H}_0| \approx 2k_F \,.$$

The real-space representation of this anomaly, in terms of $K = |\vec{k}-\vec{H}_0| - 2k_F$ is, clearly,

$$\frac{\partial D^0(k)}{\partial k}\bigg|_{K\approx 0} \sim \int_{Bz} d^3Q\left(\Omega_0(2\pi)^{-3}\sum_{l=1}^{L} e^{i\vec{Q}\cdot\vec{R}_l}\right)\ln\left(\frac{|\vec{Q}+\vec{K}|}{2k_F}\right),$$

where the integral is over the first zone, translated in this case by $\vec{H}_0$, and the sum over lattice sites extends to some finite radius R_L. The Kohn anomaly is folded with a finite-lattice diffraction pattern, and since the anomaly is integrable, the actual infinity at $K = 0$ disappears. We may evaluate this contribution approximately by changing the integration variable to $(\vec{Q}+\vec{K})$ and recognizing that

because the difference between the k values of interest and $2k_F$, namely, K, is small compared to the dimensions of the first zone, we make a small error in neglecting the concomitant change of the region of integration. Then approximating the zone with a sphere of radius q_m we find

$$\left.\frac{\partial D^0(k)}{\partial k}\right|_{K\approx 0} \sim \frac{\Omega_0}{2\pi^2}\sum_{l=1}^{L} R_l^{-3}\left[(\sin x - x\cos x)\times \ln\left(\frac{q_m}{2k_F}\right) + \sin x - \mathrm{Si}(x)\right] e^{i\vec{K}\cdot\vec{R}_l} ,$$

where $x = q_m R_l$, and Si is the sine-integral function. The asymptotic term is in R_l^{-2}; the convergence is poor for all K and becomes worse as $K \to 0$. We would expect then that the real-space sum would obliterate any Kohn anomaly.

It is interesting to speculate that a combination of real- and reciprocal-spaces method, similar to Kellermann's method for the Coulomb sum, might be devised to obviate the slow convergence of the individual real- and reciprocal-space band-structure sums. The Kellermann sum, like the Ewald sum, can be derived by writing the inverse of the interionic distance, R^{-1}, as the integral of a Gaussian, breaking the line of integration into two parts, and summing one part in reciprocal space and the other in real space. Analogously, one might write the factor R^{-1} in (2.3) as the integral of a Gaussian and separate. The real-space force constants then decay as $e^{-\epsilon^2 R^2}$, where ϵ is the integral separation point, but the reciprocal-space sum involves several difficult integrals, none of which appears to be analytically tractable. Alternatively, one might write R^{-1} as

$$\int_0^{\epsilon} e^{-pR}\,dp + \int_{\epsilon}^{\infty} e^{-pR}\,dp . \qquad (2.5)$$

Summing the second integral in real space results in integrals similar to those of (2.3) for $\mathcal{R}_l$ and $\mathcal{T}_l$ multiplied by the damping factor $e^{-\epsilon R}$. The reciprocal-space sum of the first integral in (2.5) becomes that of Eq. (2.4) with $C(K)$ replaced by

$$C'(K) = -\frac{K}{\pi}\,\mathrm{Im}\int_0^{\infty}\frac{dq}{q}\,C(q)\left(\frac{1}{q-K-ip}+\frac{1}{q+K+ip}\right)\Bigg|_{p=0}^{p=\epsilon} .$$

Unfortunately, the reciprocal-space sum in this form appears to converge no faster than the original sum and one must look elsewhere for an improved computational method.

III. MODEL INTERACTIONS

For a local bare pseudopotential v_b, the band-structure contribution to the interionic potential to second order in the pseudopotential is the energy of a bare ion interacting with the screening charge of a second ion:

$$V^{bs}(R) = (2\pi)^{-3}\int \rho_s(-q)v_b(q)e^{i\vec{q}\cdot\vec{R}}\,d^3q . \qquad (3.1)$$

In the static approximation the Fourier transform of the screening number density is

$$\rho_s(q) = \frac{-q^2}{4\pi e^2}\,v_b(q)\frac{\chi(q)}{1+[1-G(q)]\chi(q)} , \qquad (3.2)$$

where $\chi(q)$ is the Lindhard expression for the free-electron susceptibility:

$$\chi(q) = \frac{4}{\pi a_0 k_F}\frac{1}{y^2}\left(\frac{1}{2}+\frac{4-y^2}{8y}\ln\left|\frac{2+y}{2-y}\right|\right) . \qquad (3.3)$$

Here $y = q/k_F$, and a_0 is the Bohr radius. The charge density includes a static term $G(q)$ as suggested by Hubbard[43] to correct approximately for the effects of exchange and correlation. From (3.2), (3.1), and (2.1) the final expression for the C function then becomes

$$C(q) = \left(\frac{q^2}{4\pi Ze^2}\right)^2 v_b^2(q)\,\frac{\chi(q)}{1+[1-G(q)]\chi(q)} .$$

The interionic potential and elastic properties depend jointly on the bare pseudopotential and the susceptibility. The remainder of this paper will be concerned principally with three models for $C(q)$. Models A and B are those of Wallace[24]; model C includes the correction function $G(q)$ calculated by Toigo and Woodruff[44] by conserving moments of the spectral representation of the density-density Green's function in decoupling the equation of motion for the Green's function.

Model A. The Ashcroft model potential[45] is

$$v_b(r) = (-Ze^2/r)\,\theta(r-r_c) ,$$

$$v_b(q) = -4\pi Ze^2\cos(qr_c)/q^2 ,$$

where θ is the unit step function, with a core radius $r_c = 1.117a_0$ (= 0.591 Å), and a correction function $G(q)$ such that the limit of $q^2\chi(q)$ as q vanishes satisfies the compressibility sum rule with the Nozières and Pines interpolation formula.[46,47]

Model B. The Harrison model potential[48] is

$$v_b(r) = -Ze^2/r + (\beta/8\pi\rho^3)e^{-r/\rho} ,$$

$$v_b(q) = -4\pi Ze^2/q^2 + \beta/(1+q^2\rho^2)^2 ,$$

with $\beta = 47.5a_0^3$ Ry and $\rho = 0.24a_0$. The $G(q)$ is the same as that of model A. (The form factors of the model crystal potential given by Wallace differ by a factor of N/Ω from the Fourier transforms of the single-ion local model potentials A and B because there are N identical ion sites and the plane wave functions are normalized to the crystal volume.)

Model C. This is the Harrison model potential with $\beta = 49.0a_0^3$ Ry and $\rho = 0.27a_0$. These parameters provided the best fit to the experimental phonon en-

ergies when the correction function of Toigo and Woodruff was used. Much has been written about the $G(q)$ function[49]; in this paper it seems appropriate only to remark that the Toigo-Woodruff function satisfies a number of criteria deduced on general theoretical grounds. It predicts an electron pair correlation function $g(r)$ which remains positive at $r=0$ for $r_s<3$ (for Al $r_s=2.073$). At $r_s=3$ the pair correlation function is nearly identical to the most recent results of Singwi *et al.* (IV).[50] The function $G(q)/q^2$ has the limit $\frac{1}{4}$ for small q, resulting in close agreement between the compressibility calculated from thermodynamics and that found from the compressibility sum rule.[51] The function $G(q)/q^2$ also has a small hump at $q \lesssim k_F$ as suggested by the approximate Hartree-Fock diagram summation of Geldart and Taylor.[52]

The bare-ion model potential and electron-gas susceptibility are the necessary ingredients not only for a calculation of the screening charge density and ion-electron-ion interaction, but also for a calculation of the conduction electron-ion interaction $v(q)$. For the latter interaction, however, some account must be taken of the fact that the conduction electron may exchange with the electrons of the screening cloud. (The bare ion of the former interaction obviously cannot so exchange.) In this case $v(q)=v_b(q)\,\Lambda(q)$,[49] where the vertex function $\Lambda(q)$ is given by

$$\Lambda^{-1}(q)=1+[1-G(q)]\chi(q)\ .$$

If one wishes to ascribe physical significance to a model potential, one must demonstrate that it correctly predicts diverse effects of the interaction $v(q)$, such as the energy band structure and the electrical resistivity of the melt. We wish here to make the observation that both the Ashcroft potential of model A and the Harrison potential of models B and C are somewhat unsatisfactory for the former in Al. Because the free-electron energy for wave vectors near W is considerably closer to the free-electron Fermi energy than is the energy of other wave vectors, the band splittings at W significantly affect the Fermi surface. Ashcroft[53] has considered a wide variety of Al de Haas–van Alphen data from which he has determined the two potential parameters in a four-pseudo-plane-wave model $V_{111}=0.0179$, $V_{200}=0.0562$ Ry. These parameters lead to a splitting of the energy bands at the W point labeled "expt" in Table I. The reciprocal lattice of the fcc crystal has the point symmetry D_{2d} about the W point $2\pi(1, \frac{1}{2}, 0)/a$, where the major symmetry axis is in the y direction, the two mirror planes are xy and zy, and the twofold rotation axes are in the $(x+y)$ and $(x-y)$ directions. The successive stars of vectors $(\vec{H}-\vec{k}_W)$ of increasing length contain 4, 4, 8, $8+4=12$, etc., reciprocal-lattice vectors at $|\vec{H}-\vec{k}_W|^2/(4\pi^2a^{-2})=1.25$, 3.25, 5.25, 7.25, etc. Four-pronged stars occur when one of the components of $(\vec{H}-\vec{k}_W)$ is zero and are formed by the subset of D_{2d} operations which leave the sign of one component unchanged. Accordingly, we have calculated the energy-band splitting using four-, eight-, and sixteen-pseudo-plane-wave models and find that the results, shown in Table I, are poorly convergent because of a volatile W_1 point. As one increases the number of plane waves, the calculations become more time consuming and the results less physically meaningful as one represents in ever greater detail the core region of the potential as described by the model. By contrast the potential of Heine and Animalu[54] leads to rapid convergence and reasonable agreement with experiment. The potentials of models A, B, and C closely resemble that of Heine and Animalu in the region of the first node and first several reciprocal-lattice vectors, and they give similar values for the parameters V_{111} and V_{200}, although the node of model C occurs at a wave vector which is slightly larger than the first reciprocal-lattice vector, leading to an inversion of the order of W_1 and W_2' energies in the four-pseudo-plane-wave model. For comparison we have calculated the values of Harrison model-potential parameters required to fit exactly the experimental values of V_{111} and V_{200} in the four-pseudo-plane-wave model. Using the vertex correction of model B requires $\beta=59.4a_0^3$ Ry and $\rho=0.330a_0$; using the vertex correction of model C requires $\beta=62.8a_0^3$ Ry and $\rho=0.357a_0$.

TABLE I. Splittings of the energy bands at W in units of rydbergs. The experimental splitting is from Ashcroft's analysis in Ref. 53. Models A and C calculations are for four, eight, and sixteen pseudo plane waves. The W_3 value is twofold degenerate by symmetry.

		$W_1 - W_2'$ (Ry)	$W_2' - W_3$ (Ry)
1	ΨPW	0	0
Expt		0.0716	0.0766
Model *A*			
4	ΨPW	0.0178	0.0993
8		0.0182	0.0828
16		−0.0126	0.0880
Model *C*			
4	ΨPW	−0.0017	0.1046
8		0.0032	0.0867
16		−0.0259	0.0939

No convergence problem plagues the calculation of the scattering on the Fermi surface for the electrical resistivity at the melting point. Using the Ziman[55] liquid-metal formula with the hard-sphere model[56] for the structure factor, a packing fraction of 0.45, and a density of 2.380 g/cm^3, we find the results of Table II. The peak of the hard-sphere structure factor occurs at $q/2k_F=0.803$, which is within 0.05 Å^{-1} of the first node of the model po-

TABLE II. Electrical resistivity in $\mu\Omega$ cm of liquid Al at the melting point 660 °C. The experimental value is from Ref. 57. Theoretical values are all calculated with the hard-sphere structure factor for the three model potentials of the text and for the model potential of Heine and Animalu (HA).

Expt	Model A	B	C	HA
24.2	20.2	21.2	20.3	20.6

tential in each case. This near coincidence leads to a low value of the resistivity, which increases if the node is moved to larger values of q. Complete agreement between theory and experiment cannot be expected because of the approximate nature of the structure factor and because of possible changes with Fermi energy in the model-potential parameters as the atomic volume is increased by 13% of the solid value between zero degrees and the melting point. Such energy dependences might be introduced by fitting the liquid thermopower, but such an attempt was not made here.

IV. PHONON CALCULATIONS

In fitting a model potential to phonon energies, particularly when the dynamical matrix is constructed in real space, it is convenient to begin with the second moment of the phonon spectrum, which can be found by taking the trace of $D_{\alpha\beta}(\vec{k})$. An expression for $\langle\omega^2\rangle$ derived from the reciprocal-space sum has been given by Wallace.[9] In terms of real-space parameters

$$\langle\omega^2\rangle = (3M)^{-1}\sum_l (\mathcal{R}_l + 2\mathcal{T}_l)$$

$$= \left(\frac{2Z^2e^2}{3\pi M}\right)\int_0^\infty C(q)q^2\sum_l \frac{\sin(qR_l)}{qR_l}\,dq\,, \qquad (4.1)$$

TABLE III. Second moments of the phonon spectrum in units of 10^{25} (rad/sec)^2. The first column of theoretical values has been calculated from 21 shells of real-space force constants (uncorrected) with the models described in the text. The second column results from 114 shells with the correction of Eq. (3.2).

	$\langle\omega^2\rangle_0$ [10^{25} rad/sec)^2]	$\langle\omega^2\rangle$ [10^{25} rad/sec^2]
Specific heat (Ref. 59)	166	
Interpolation (Ref. 59)	171[a]	
Model A	163	161
B	164	161
C	169	167

[a]This value is computed from a phonon density of states derived from the eight-shell model at 80 °K.

TABLE IV. Calculations of the second moment of the energy spectrum from model A. Units are 10^{25} (rad/sec)^2. $\langle\omega^2\rangle_0$ is the uncorrected value from Eq. (3.1); $\langle\omega^2\rangle$ includes the correction of Eq. (3.2). The deviations in parentheses indicate the size of the $(2k_F)^{-1}$ oscillations at each shell radius. Inside shell No. 114 there are 3588 lattice vectors.

Shells	R_L (Å)	$\langle\omega^2\rangle_0$(10^{25} rad^2/sec^2)	$\langle\omega^2\rangle$(10^{25} rad^2/sec^2)
8	8.098	166 (+1, −6)	165 (+3, −4)
21	12.147	163 (+1, −2)	162 (+1, −2)
114	24.294	161 (+1, −1)	161 (+½, −0)

where M is the ionic mass. The sum over lattice sites l extends to some finite number L, and a plot of $\langle\omega^2\rangle$ as a function of L provides a measure of the convergence of the real-space sum for phonon energies. Since, however, both ω^2 and the spectrum are largest for large frequencies where the convergence appears to be best, the damped oscillations in $\langle\omega^2\rangle$ vs R_L, of asymptotic periodicity $(2k_F)^{-1}$, provide an approximate lower bound for the fluctuations in phonon energies. For actual calculations of $\langle\omega^2\rangle$, convergence can be improved for large R_L by adding a correction term calculated by approximating the sum in (4.1) from radius R_L to infinity with an integral. We find the correction term to be simply

$$\Delta\langle\omega^2\rangle = -(4\pi N/3M\Omega)R_L^3\mathcal{T}_L\,.$$

TABLE V. Radial and tangential force constants in units of dyn/cm. $\mathcal{R}$ and $\mathcal{T}$ are calculated from model C. Those shells with no entry have the same radius, and thus the same force constants, as the previous shell. The last two columns are the force constants of the eight-shell model obtained in Ref. 59 by fitting the 80 °K experimental phonon dispersion curves of Refs. 60 and 61.

Shell	Type	$\mathcal{R}$ (dyn/cm)	$\mathcal{T}$ (dyn/cm)	$\mathcal{R}^{GN}$ (dyn/cm)	$\mathcal{T}^{GN}$ (dyn/cm)
1	110	21 280	−1 273	21 551	−1 337
2	200	3 468	− 218	2 452	−529
3	211	−1 190	63	−921	−33
4	220	341	−46	221	321
5	310	285	22	491	198
6	222	−453	1	−76	251
7	321	131	−13	−34	−118
8	400	232	5	−534	−116
9	330	−153	6		
10	411	···	···		
11	420	−142	−4		
12	332	108	−4		
13	422	121	1		
14	431	−51	3		
15	510	···	···		
16	521	−8	−3		
17	440	85	−1		
18	433	56	1		
19	530	···	···		
20	442	−33	2		
21	600	···	···		

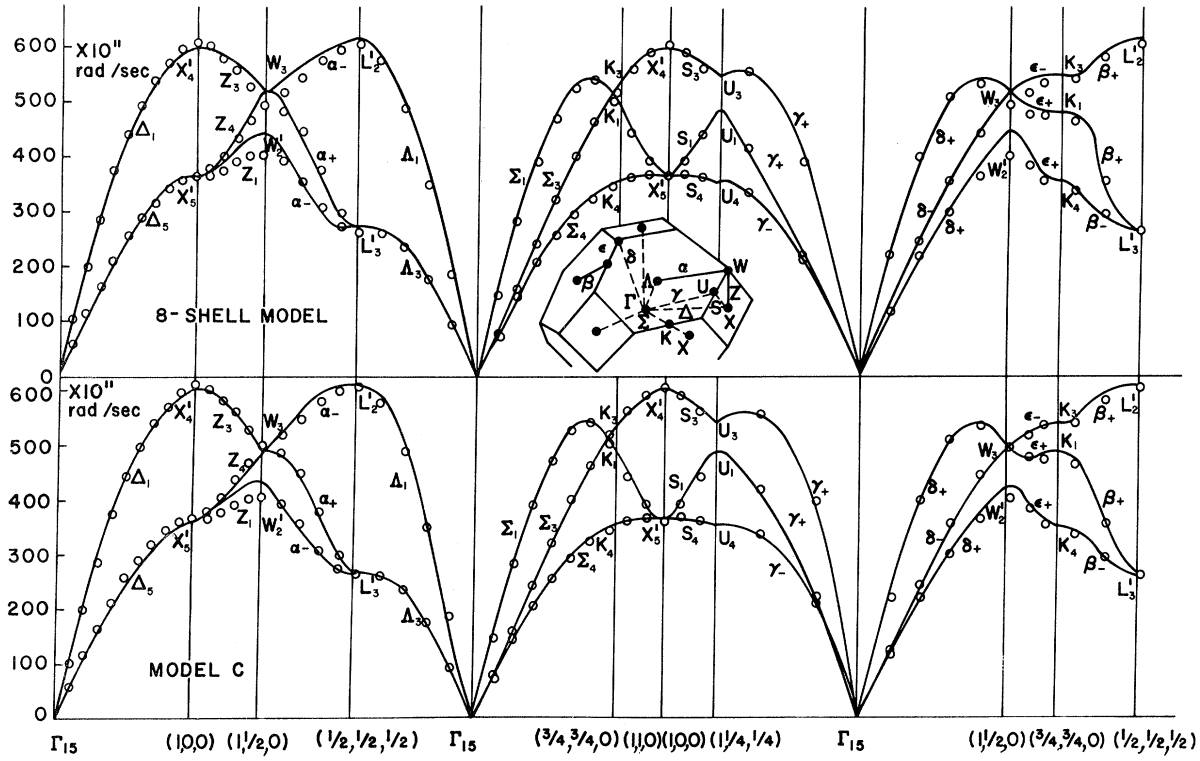

FIG. 1. Calculated and experimental phonon dispersion relations. The solid line in the top half of the figure is calculated from the eight-shell model, that in the lower half of the figure from model *C*. Experimental points (circles) in both halves are the 80 °K measured and interpolated energies of Stedman and co-workers.

Experimental and calculated values of the second moment appear in Table III. An example of the convergence of the second moment is given for model *A* in Table IV.

The interionic potential and force constants were calculated by performing the integrals of Eq. (2.3) to $34k_F$ with Simpson's rule at 2400 points. The interionic potential for both models *A* and *B* shows the double minimum noted by Ashcroft and Langreth[58] for model *A*. The first zero crossings, at 2.7 and 2.9 Å, respectively, and the minima occur at approximately the same interionic distances, but the first minimum of model *B* shows only 40% of the depth of that of model *A*. The interionic potential calculated from model *C* crosses zero at 4 Å and has a single minimum at 4.3 Å, close to the second minimum of models *A* and *B*. The interionic potentials for the three models are essentially the same for $R > 7$ Å. Although the interionic potential is extremely sensitive to the model chosen, its derivatives are relatively stable, and the radial and tangential force constants, given in Table V for model *C*, are rather similar for all three models.

Phonon dispersion curves calculated from the eight shells of force constants of Ref. 59 and from model *C* are shown in Fig. 1 along with the experimental and interpolated points of Stedman and Nilsson.[60,61] Models *A* and *B* result in dispersion curves which agree only slightly less well with experiment; the differences cannot be easily seen on the scale of the figure, and they can scarcely be considered as physically meaningful in view of the finite temperature of the experiment and the error of approximately 2% resulting from truncation of the real-space sum at 21 shells. The labeling of symmetry points and of the irreducible representations follows that of Bouckaert *et al.*,[62] except for five lines α, β, γ, δ, and ϵ for which the group of the wave vector contains only the identity and one other element, respectively, C_2', JC_2', JC_2', JC_4^2, and JC_4^2. Because these small groups have only even and odd irreducible representations, one of them must occur at least twice. However, neither can occur three times, for in that case the character of the nonidentity element of the small group in a three-dimensional direct-sum representation would be ± 3. Because the representations are unitary, such a character can occur in a three-dimensional representation only for the identity and the inverse, neither of which is different from the identity element in the five small groups above. Therefore, one irreducible representation occurs twice and the two phonon polarization vectors which

transform according to the repeated irreducible representation are not entirely determined by symmetry but depend on the phonon wave vectors and energies.

Models A, B, and C result in crossings of Σ, Z, and γ lines all at approximately the same wave vector, whereas the fitted eight-shell force constants predict a crossing only along Σ. The largest discrepancy between calculation and experiment, as well as between models A, B, and C and the eight-shell model, is at the point W. Our models miss the experimental W_2' point; the eight-shell model badly misses both W_2' and W_3 points by 11 and 4%, respectively, as previously noted by Stedman *et al.*[63] The relatively bad agreement at W persists along the symmetry lines which include W.

Further comparison of theoretical and 80 °K experimental phonon energies can be made over the whole Brillouin zone. Stedman kindly sent us a table of 480 measured and interpolated phonon energies of which 449 are independent by symmetry. By performing the real-space sum for 155 uniformly spaced wave vectors, we found the percentage error distributions of Fig. 2. The error distributions for models A and B are quite similar and have been averaged in the figure. The larger errors >4% for models A, B, and C are in the energies of phonons with small wave vectors, where the small experimental phonon energy leads to large percentage errors. The elastic constant calculations of Wallace lead us to expect relatively poor agreement at low k, though it must also be said that the convergence of our calculations becomes increasingly poor with decreasing k. By contrast, the small wave-vector energies of the eight-shell-model calculation are in excellent agreement with experiment, probably because the force-constant fitting procedure required agreement with measured elastic constants. The relatively large errors from the eight-shell model, then, come from the middle of the zone. At the very least, therefore, we may claim that for Al the two-parameter model potential, fitted in our calculations to the Σ phonons, provides a better over-all interpolation scheme than does the sixteen-parameter application of the standard force-constant fitting procedure. Although the error distribution for model C appears to be sharper than that for models A and B, the uncertainties in both calculations preclude a claim that the Toigo-Woodruff susceptibility function results in agreement with experiment which is actually better than the excellent agreement achieved by Wallace. It is, however, gratifying that the new susceptibility function can do at least as well.

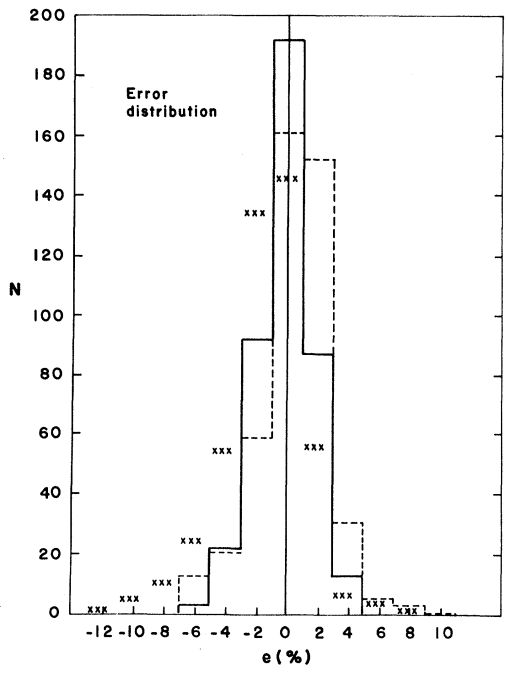

FIG. 2. Percentage error distribution $N(e)$ is the number of calculated phonon energies out of 449 which differ from the experimental energies by a percentage of the experimental value which lies in the range $e \pm 1$. The short dashed line is the eight-shell model, the solid line is model C, and the line of crosses gives the average of models A and B.

Although further comparison of harmonic calculations with experiments at large wave vectors seems pointless, it is interesting to compare models A and B with one another. Wallace[24] found that although the model potentials A and B differed considerably for $q > 2k_F$, the phonon energies calculated from the two potentials were essentially the same along the three principal symmetry directions. Our calculations show that this quite remarkable agreement extends over the whole Brillouin zone. Moreover, the agreement persists for phonon wave vectors so small (several orders of magnitude smaller than are observed in neutron scattering) that 21 shells of force constants are inadequate to achieve reliable energies. For quantitative comparison of various calculated quantities we increased the core radius of model A by less than 1% to 0.594 Å. The resulting changes in phonon energies for large k are two to four times the differences in energies calculated from models A and B. In the discussion to follow, large differences between models A and B will mean large compared to the corresponding changes induced by the above modification of the core radius of model A. In brief, the difference $\Delta C(q)$ between the $C(q)$ functions of models A and B is a function with a large broad peak centered at 6 Å^{-1} with a half-width of 2 Å^{-1}. The peak results in large oscillatory differences in the interionic potential and, from the derivative expressions, large differences in the

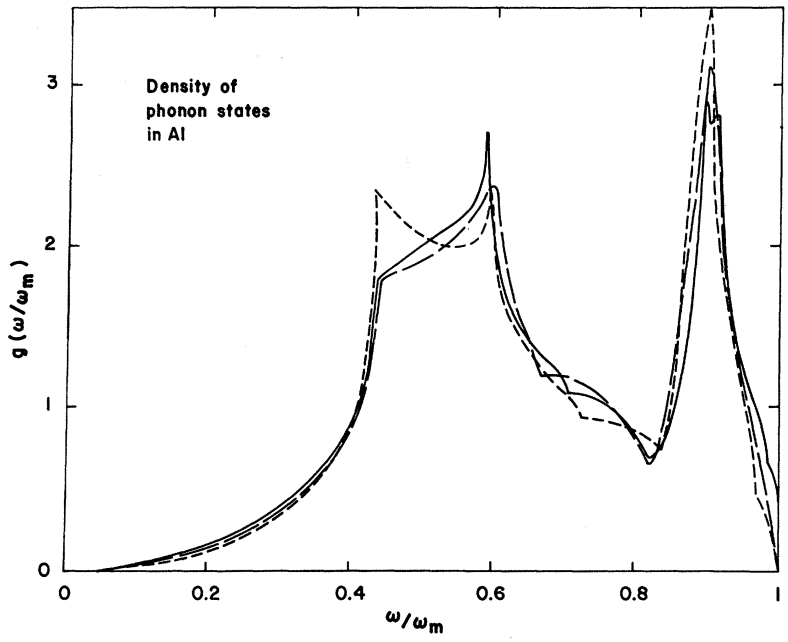

FIG. 3. Normalized densities of phonon states for Al. Short dashed line is calculated from the eight-shell model; long dashed line is the interpolated curved traced from Ref. 63. Solid line is calculated from 21 shells of force constants of model C. Maximum frequencies occur at the L point and are, respectively, 618, 606 (experimental), and 612×10^{11} rad/sec.

radial and tangential force constants. When radial and tangential force constants are combined into the Squires[64] form, the differences are still large. When the Squires-type matrices are finally summed to form a dynamical matrix, the differences become small for almost all values of $\vec{k}$. It appears to us, therefore, that the explanation for the extraordinary agreement between the phonon energies of models A and B is not to be found in real space. The solution to this puzzle might be found, instead, by analyzing the reciprocal-space sum for the difference function $\Delta C(q)$.

The real-space calculation makes it relatively easy to calculate lattice properties which depend only on the normal-mode energies. In Fig. 3 the density of states is plotted. As expected, the density of states calculated from model C agrees better with the visually interpolated curve than does that calculated from the eight-shell model. In Fig. 4 the specific-heat Θ_D function is plotted. The agreement between theory and experiment is excellent above 20 °K, but unfortunately the convergence difficulties for long-wavelength phonons precluded accurate calculations of the specific heat at the lower temperatures of the experimental hump.

These convergence difficulties in the long-wavelength limit are easily understood. The first term in a Taylor's expansion of the dynamical matrix $\overleftrightarrow{D}(\vec{k})$ about $k=0$ is of order k^2, which introduces an extra factor of R_l^2 into the sum. Because the envelopes of $\mathcal{R}_l$ and $\mathcal{T}_l$ decay asymptotically as R_l^{-5} and the density of lattice sites increases as R_l^2, the resulting sum converges only as R_l^{-1} for small k. For example, the calculated longitudinal energy at $q=2\pi(0.3, 0, 0)/a$ changes by 1% as the number of shells is decreased from 21 to 17, whereas at wave vector $2\pi(0.03, 0, 0)/a$ and below, the longitudinal energy changes by 6%. Further, the rate of convergence is somewhat different for different lattice modes. It therefore becomes extremely difficult to calculate elastic constants by the method of long waves from a real-space sum. If one calculates c_{11}, for example, from the first eight shells of force constants[18] using the expressions of Squires,[68] the oscillations in the final value at the

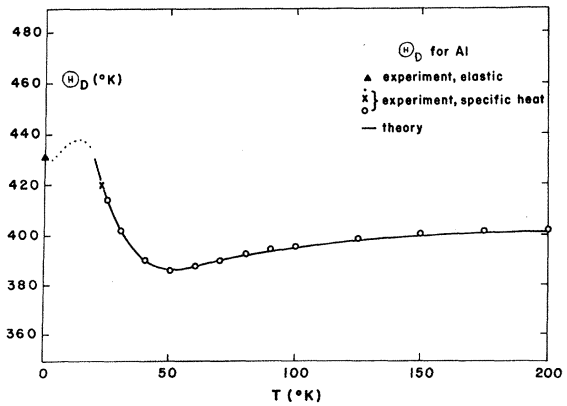

FIG. 4. Θ_D representation of the lattice specific heat for Al. Experimental points are: ▲, from elastic measurements of Ref. 65; ●, from specific-heat measurements of Ref. 66; ×, from specific-heat measurements of Ref. 67; ○, from specific-heat measurements as analyzed in Ref. 26. Solid line has been calculated from model C.

radius of the eighth shell are about 25% of the mean. Because only long-wavelength modes contribute to the low-temperature lattice specific heat, a calculation of $\Theta_D(T)$ requires an increasing number of shells of real-space force constants as T decreases. The following example illustrates the sensitivity of $\Theta_D(T)$ at low temperature to relatively long-range forces. Using the eight-shell model, Gilat and Nicklow find $\Theta_D(0) = 428\ ^\circ\mathrm{K}$. Removing the eighth shell increases the value to 481 °K, and removing both seventh and eighth shells results in a value of 625 °K. In our case the poor convergence at $k \leq 2\pi(0.03)/a$, for which transverse-phonon energies are approximately 25×10^{11} rad/sec, places a lower limit of 20 °K on the calculations of the specific heat.

A similar difficulty arises in a calculation of the crystal stability. If one assumes that the crystal energy E_c is derived entirely from the interionic pair potential, the condition that the crystal be stable against changes in lattice parameter a is

$$\frac{\partial}{\partial a} E_c = \frac{1}{a} \sum_l R_l^2 \mathcal{T}_l = 0 \sim (c_{12} - c_{44}), \tag{4.2}$$

and the sum is poorly convergent. By contrast, the reciprocal-space sum converges well; e.g., for the band-structure term Eq. (4.2) becomes

$$\frac{\partial}{\partial a} E_c^{\mathrm{bs}} = \frac{-6(2\pi)^4 N Z^2 e^2}{\Omega a} \sum_{\vec{H}} \frac{C(H)}{H^2} \quad .$$

For a complete calculation one must add to E_c the energy of the interacting electron gas and the Hartree energy as discussed by Ashcroft and Langreth.[69] Of these terms Price *et al.*[16] concluded that the derivatives of the electrostatic energy and of the Hartree energy are the largest and that stability should require (for fcc, bcc, or hcp)

$$\frac{\partial E}{\partial r_s} = \frac{1.792 Z^{5/3}}{r_s^2} - \frac{9 Z r_c^2}{a_0^2 r_s^4} \approx 0$$

with the Ashcroft potential. The expression for the Harrison potential is the same with $Z r_c^2$ replaced by $\beta/4\pi a_0 (e^2/2a_0)^{-1}$. For models A, B, and C we find, as did Price *et al.*, that the Hartree term is too small in magnitude by 20–40%. It is interesting to note, however, that from model A we find $Z r_c^2/a_0^2 = 3.74$, and the corresponding expression from model B is 3.78. This suggests that one might determine the parameters of a Harrison model potential from the Ashcroft potential by first fitting the node and then requiring the above correspondence.

It is perhaps worth mentioning that the real-space method could be used for calculating phonon lifetimes τ_q against decay into an electron-hole pair. The radial and tangential force constants become complex with an imaginary part which, in the standard approximations for this effect,[70,71] is proportional to the vibrational frequency, as expected for a viscous damped spring. The eigenvalues of the imaginary part of the dynamical matrix are $-2\omega_q/\tau_q$, and therefore the lifetimes may be calculated from the imaginary part of the dynamical matrix independently of the phonon energies. However, the recipocal-space sum provides a simpler calculation for phonon lifetimes because the imaginary part of the susceptibility $\chi(q)$ vanishes for $q > 2k_F$ for phonon velocities less than a critical value.[72] The ratio of the Bohm-Staver speed of sound to the critical velocity is $O(m/M)^{1/2}$, and the criterion is satisfied for metals.

V. DISCUSSION

Despite the limitations which we have noted, we consider the real-space method of phonon-energy calculations to be a practical alternative to the conventional reciprocal-space method if one is more interested in accurate sampling of the entire Brillouin zone than in faithful reproduction of rapid variations at anomalous points. We have used the real-space method to demonstrate that with an appropriate choice of model potential (model C) the theoretically attractive Toigo-Woodruff susceptibility function results in excellent agreement between calculated and experimental phonon energies.

The agreement, of course, provides no definitive test of either the susceptibility function or model potential. Among the aspects of the problem which have been neglected in this work are the contributions to phonon energies to higher order than the second in the model potential. There are fourth-order terms, for example, with the simple physical interpretation of nonsphericity of the screening charge distribution due to neighboring ions, directly related to the nonsphericity of the Fermi surface. Classically, the effect of these asymmetries might be estimated by allowing the Fermi wave vector in the Lindhard function to depend upon wave-vector direction, thus fitting the Kohn anomalies to the measured Fermi-surface dimensions. The Fermi surface of Al is distorted from the free-electron sphere, at least to the extent that the fourth-band states disappear. Furthermore, the phonon energies are rather sensitive to the Fermi wave vector. Increasing k_F by 1% in model C results in a change of at least −4% in all 449 phonon energies calculated and of −10% for a number of phonons of large and intermediate wave vector. It seems quite likely that the effects of Fermi-surface distortion will appreciably alter the phonon energies.

ACKNOWLEDGMENTS

We wish to thank Dr. R. Stedman for a table of experimental and interpolated phonon energies and to thank Dr. F. Toigo, Dr. T. O. Woodruff, and Dr. D. C. Wallace for helpful discussions.

*Work partially supported by National Science Foundation under Science Development Grant No. GU 2648.

†National Science Foundation Predoctoral Fellow.

[1]T. Toya, J. Res. Inst. Catalysis, Hokkaido Univ. 6, 183 (1958).

[2]W. Cochran, Proc. Roy. Soc. (London) A276, 308 (1963).

[3]L. J. Sham, Proc. Roy. Soc. (London) A283, 33 (1965)

[4]W. M. Shyu and G. D. Gaspari, Phys. Rev. 163, 667 (1967).

[5]T. Schneider and E. Stoll, Physik Kondensierten Materie 6, 135 (1967).

[6]D. C. Wallace, Phys. Rev. 176, 832 (1968).

[7]N. W. Ashcroft, J. Phys. C 1, 232 (1968).

[8]P. S. Ho, Phys. Rev. 169, 523 (1968).

[9]D. C. Wallace, Phys. Rev. 176, 832 (1968).

[10]S. Prakash and S. K. Joshi, Phys. Rev. 185, 913 (1969).

[11]S. Prakash and S. K. Joshi, Phys. Rev. 187, 808 (1969).

[12]D. C. Wallace, Phys. Rev. 178, 900 (1969).

[13]D. C. Wallace, Phys. Rev. 182, 778 (1969).

[14]D. J. W. Geldart, R. Taylor, and Y. P. Varshni, Can. J. Phys. 48, 183 (1970).

[15]L. Martinelli, Nuovo Cimento 70, 58 (1970).

[16]D. L. Price, K. S. Singwi, and M. P. Tosi, Phys. Rev. B 2, 2983 (1970).

[17]A. O. E. Animalu, F. Bonsignori, and V. Bortolani, Nuovo Cimento 44, 159 (1966).

[18]W. M. Shyu and G. D. Gaspari, Phys. Rev. 170, 687 (1968).

[19]T. Schneider and E. Stoll, Physik Kondensierten Materie 5, 331 (1966).

[20]T. Schneider and E. Stoll, *Neutron Inelastic Scattering* (IAEA, Vienna, 1968), Vol. 1, p. 101.

[21]M. A. Coulthard, J. Phys. C 3, 820 (1970); S. H. Vosko R. Taylor, and G. H. Keech, Can. J. Phys. 43, 1187 (1965).

[22]T. Schneider and E. Stoll, Physik Kondensierten Materie 5, 364 (1966).

[23]W. A. Harrison, Phys. Rev. 136, A1107 (1964).

[24]D. C. Wallace, Phys. Rev. 187, 991 (1969).

[25]H. C. Gupta and B. B. Tripathi, Phys. Rev. B 2, 248 (1970).

[26]D. C. Wallace, Phys. Rev. B 1, 3963 (1970).

[27]A. P. Roy and G. Venkataraman, Phys. Rev. 156, 769 (1967).

[28]J. V. Koppel and A. A. Maradudin, Phys. Letters 24A, 244 (1967).

[29]E. Stoll and T. Schneider, Physik Kondensierten Materie 8, 58 (1968).

[30]G. Gilat, G. Rizzi, and G. Cubiotti, Phys. Rev. 185, 971 (1969).

[31]P. B. Allen and M. L. Cohen, Phys. Rev. 187, 525 (1969).

[32]R. W. Shaw and R. Pynn, J. Phys. C 2, 2071 (1969).

[33]V. C. Sahni and G. Venkataraman, Phys. Rev. 185, 1002 (1969).

[34]W. F. King and P. H. Cutler, Phys. Rev. B 2, 1733 (1970).

[35]W. A. Harrison, Phys. Rev. 139, A179 (1965).

[36]T. Toya, *Lattice Dynamics* edited by R. F. Wallis (Pergamon, London, 1965), p. 91.

[37]E. G. Brovman and Yu. Kagan, Zh. Eksperim. i Teor. Fiz. 52, 557 (1967) [Sov. Phys. JETP 25, 365 (1967)].

[38]E. W. Kellermann, Phil. Trans. Roy. Soc. London A238, 513 (1940).

[39]R. M. Martin, Phys. Rev. Letters 21, 536 (1968); G. Srinivasan, Phys. Rev. 178, 1244 (1969).

[40]C. J. Pethick, Phys. Rev. B 2, 1789 (1970); L. Sham, Proc. Phys. Soc. (London) 78, 895 (1961).

[41]G. Gilat and G. Dolling, Phys. Letters 8, 304 (1964); G. Gilat and L. J. Raubenheimer, Phys. Rev. 144, 390 (1966).

[42]For example, the ideal-resistivity calculations of R. Dynes and J. Carbotte, Phys. Rev. 175, 913 (1968).

[43]J. Hubbard, Proc. Roy. Soc. (London) A243, 336 (1957).

[44]F. Toigo and T. O. Woodruff, Phys. Rev. B 2, 3958 (1970).

[45]N. W. Ashcroft, Phys. Letters 23, 48 (1966).

[46]D. Pines and P. Nozières, *The Theory of Quantum Liquids* (Benjamin, New York, 1966), Vol. 1.

[47]D. J. W. Geldart and S. H. Vosko, Can. J. Phys. 44, 2137 (1966); 45, 2229E (1967).

[48]W. A. Harrison, *Pseudopotentials in the Theory of Metals* (Benjamin, New York, 1966), p. 298ff.

[49]See, for example, R. W. Shaw, J. Phys. C 3, 1140 (1970).

[50]K. S. Singwi, A. Sjolander, M. P. Tosi, and R. H. Land, Phys. Rev. B 1, 1044 (1970).

[51]L. Hedin and S. Lundquist, *Solid State Physics*, edited by F. Seitz, D. Turnbull, and H. Ehrenreich (Academic, New York, 1969), Vol. 23.

[52]D. J. W. Geldart and R. Taylor, Can. J. Phys. 48, 155 (1970).

[53]N. W. Ashcroft, Phil. Mag. 8, 2055 (1963).

[54]A. O. E. Animalu, Phil. Mag. 11, 379 (1965); D. Brust, Phys. Rev. B 2, 818 (1970); A. O. E. Animalu and V. Heine, Phil. Mag. 12, 1249 (1965).

[55]J. M. Ziman, Phil. Mag. 6, 1013 (1961). Although the Ziman formula does not depend on the pseudopotential at q values greater than $2k_F$, there is considerable doubt as to the convergence of the expansion in the pseudopotential itself, which, for the Ziman formula is terminated at the Born term; cf. N. W. Ashcroft and W. L. Schaich, Phys. Rev. B 1, 1370 (1970).

[56]N. W. Ashcroft and J. Lekner, Phys. Rev. 145, 83 (1966).

[57]N. E. Cusack, Rept. Progr. Phys. 26, 361 (1963).

[58]N. W. Ashcroft and D. C. Langreth, Phys. Rev. 159, 500 (1967).

[59]G. Gilat and R. Nicklow, Phys. Rev. 143, 487 (1966).

[60]R. Stedman and G. Nilsson, *Inelastic Scattering of Neutrons in Solids and Liquids* (IAEA, Vienna, 1965), Vol. 1, p. 211.

[61]R. Stedman and G. Nilsson, Phys. Rev. 145, 492 (1966).

[62]L. P. Bouckaert, R. Smoluchowski, and E. Wigner, Phys. Rev. 50, 58 (1936).

[63]R. Stedman, L. Almqvist, and G. Nilsson, Phys. Rev. 162, 549 (1967).

[64]G. L. Squires, *Inelastic Scattering of Neutrons in Solids and Liquids* (IAEA, Vienna, 1963), Vol. 2, p. 71.

[65]G. N. Kamm and G. A. Alers, J. Appl. Phys. 35, 327 (1964).

[66]W. T. Berg, Phys. Rev. 167, 583 (1968).

[67]W. F. Giauque and P. F. Meads, J. Am. Chem. Soc. 63, 1897 (1941).

[68]G. L. Squires, Arkiv Fysik 25, 21 (1963).

[69]N. W. Ashcroft and D. C. Langreth, Phys. Rev. 155, 682 (1967).
[70]E. J. Woll and W. Kohn, Phys. Rev. 126, 1693 (1962).
[71]G. Björkman, B. I. Lundquist, and A. Sjölander, Phys. Rev. 159, 551 (1967).
[72]T. D. Schultz, *Quantum Field Theory and the Many-Body Problem* (Gordon and Breach, New York, 1964), p. 96.

PHYSICAL REVIEW B VOLUME 3, NUMBER 12 15 JUNE 1971

Study of Thermal Diffuse X-Ray Scattering from Lead Single Crystals*†

Sanford L. Schuster
Physics Department, Mankato State College, Mankato, Minnesota 56001

and

John W. Weymouth
Behlen Laboratory of Physics, University of Nebraska, Lincoln, Nebraska 68508

(Received 21 September 1970)

Thermal diffuse x-ray scattering (TDS) from lead single crystals has been measured in the longitudinal and transverse branches along the [100] and [111] directions. In order to determine if one can use x rays to obtain reliable dispersion curves from a metal such as lead, the measured TDS was compared with that calculated from lead dispersion curves obtained by means of slow-neutron scattering. The one-phonon intensity was calculated directly from the [100] and [111] neutron data, and the two-phonon intensity was calculated by a method which expresses the cross section in terms of the atomic force constants determined by a fit to the neutron data. The intensity of the higher-order scattering was calculated by a method in which the Debye-Jauncey relation for TDS is expanded in powers of the Debye-Waller factor and the first two terms are subtracted. In addition, a very small Compton-scattering contribution was calculated. It is observed that in all cases, except for some points along the [111] transverse branch, the measured intensity is greater. The differences range from 10 to 60% or higher, and have a periodic dependence on reciprocal-lattice position. The source of this extra scattering has not yet been conclusively identified.

I. INTRODUCTION

In this paper we present the results of a study of thermal diffuse x-ray scattering (TDS) from lead single crystals along the [100] and [111] directions. The intensity of this scattering is compared with the expected intensity calculated from lead phonon dispersion curves determined by means of slow-neutron scattering.[1,2] This study was initiated in order to examine the extent to which x rays, as distinct from neutrons, can be used to obtain reliable phonon dispersion curves in a metal such as lead. The approach was to make a careful examination of the validity of the multiphonon corrections to experimentally obtained TDS data.

TDS provides an indirect approach to the determination of dispersion relations, since the dispersion relations are determined from the intensity of the total x-ray scattering. The total scattering includes not only photon–single-phonon scattering events, but also photon–multiple-phonon scattering events and Compton scattering. On the other hand,

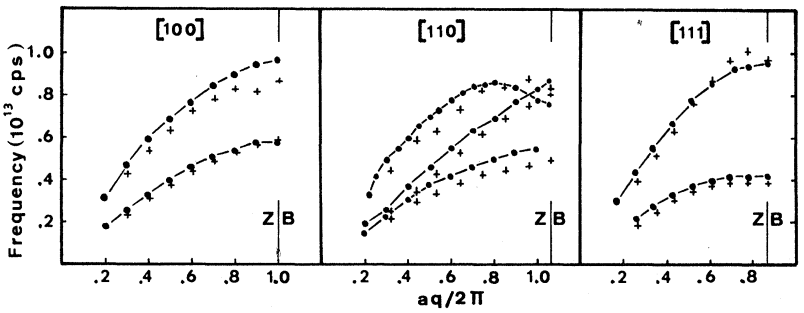

FIG. 1. Aluminum dispersion curves. -·-·-·-, neutron results from Ref. 9. +, x-ray results from Ref. 7.